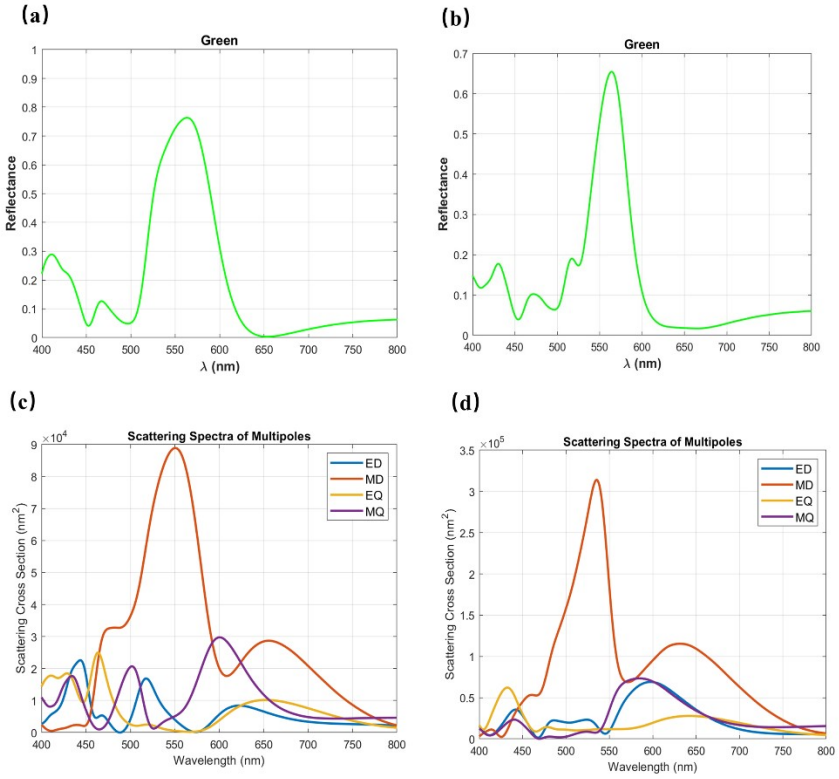

Figure S1. Multipolar decomposition and spectral analysis of the circular and elliptical nanopillars. (a) and (c): Reflection spectra and the corresponding scattering cross-sections of the multipolar components for the circular nanopillar (initial design). (b) and (d): Reflection spectra and multipolar decomposition for the elliptical nanopillar (proposed design).

The results clearly show that for both designs, the Magnetic Dipole (MD) mode is the dominant contributor to the primary resonance peak, while the Electric Dipole (ED), Electric Quadrupole (EQ), and Magnetic Quadrupole (MQ) have secondary contributions. The high-reflection characteristic is attributed to this localized magnetic Mie resonance.

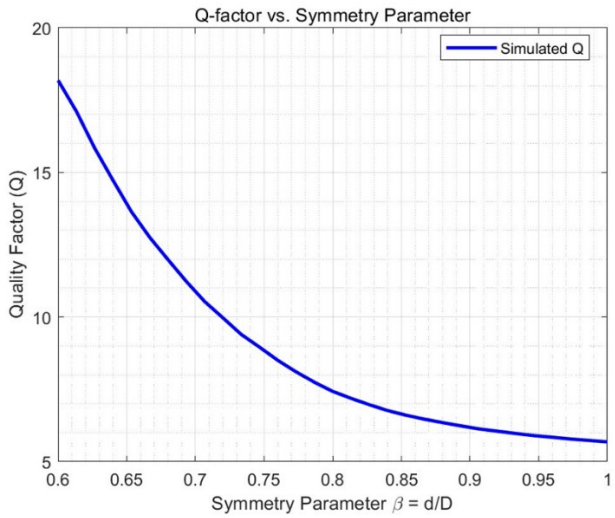

Figure S2. Analysis of the quasi-BIC mechanism via Q-factor dependence on the symmetry parameter.

The simulated Q-factor of the green-channel metasurface is plotted as a function of the **symmetry parameter** $\beta = d/D$. Here, $\beta = 1$ corresponds to the perfectly symmetric limit (circular nanopillars). his analysis was performed by sweeping the short-axis diameter d while keeping other geometric parameters (D, G, h) fixed.

The observed trend is consistent with the principles of a quasi-BIC mechanism when observed in a **reflection-mode configuration**. Traditional Q-BIC theory often describes the "internal" Q-factor, which approaches infinity as the structure becomes perfectly symmetric ($\beta \to 1$) because the mode becomes a perfectly confined "dark mode" with zero radiative loss.

However, in our reflection-based system, we measure the "external" Q-factor from the far-field reflection spectrum. At the high-symmetry limit ($\beta \approx 1$), the dark mode is effectively decoupled from free space, resulting in near-zero reflection and thus a very low observable external Q-factor. As the symmetry is broken (β decreases), a radiation channel is opened, allowing the internally confined high-Q mode to be efficiently coupled out and observed in the reflection spectrum. Therefore, the **external Q-factor increases as the asymmetry increases (i.e., as β decreases)**, which is the inverse of the behavior of the internal Q-factor. This trend confirms that our design utilizes the Q-BIC principle to activate and harvest a high-Q resonance for narrowband filtering.

It is important to note that our final design parameters presented in the main text do not necessarily correspond to the highest Q-factor shown here. The final selection is an **optimized trade-off** between achieving a high Q-factor, maintaining high peak reflectance, and ensuring the resonance wavelength aligns with the target RGB color channel.

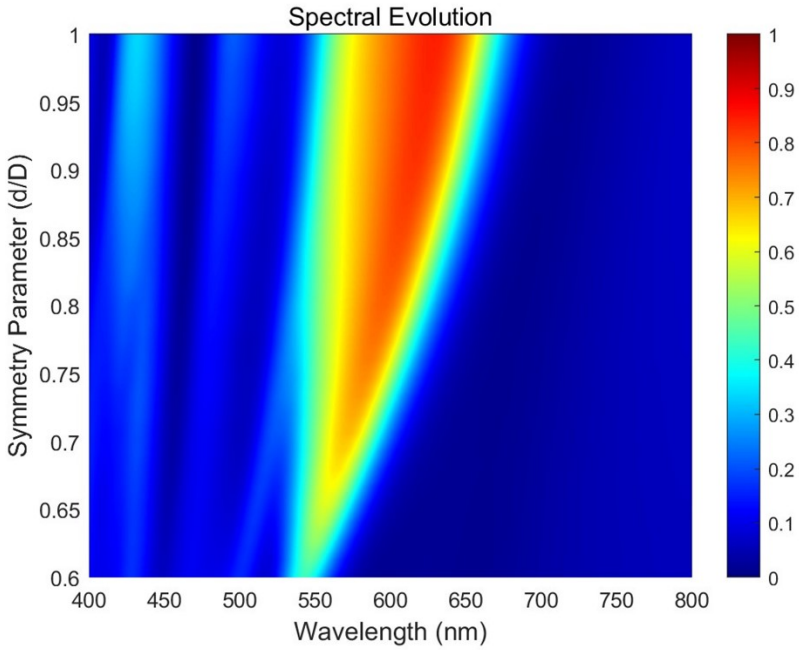

Figure S3. Spectral evolution of the metasurface as a function of the symmetry parameter.

The reflection spectra of the **green-channel metasurface** are presented as a color map, showing their evolution with respect to the **symmetry parameter (d/D)**. This parameter sweep follows the same methodology as described for Figure S2.

This visualization intuitively demonstrates the Q-BIC mechanism in reflection. As the symmetry parameter decreases (increasing asymmetry), the resonance peak becomes sharper and the linewidth significantly narrows. This corresponds to an increase in the Q-factor, highlighting how geometric tuning effectively activates and optimizes the high-Q resonance for narrowband filtering.

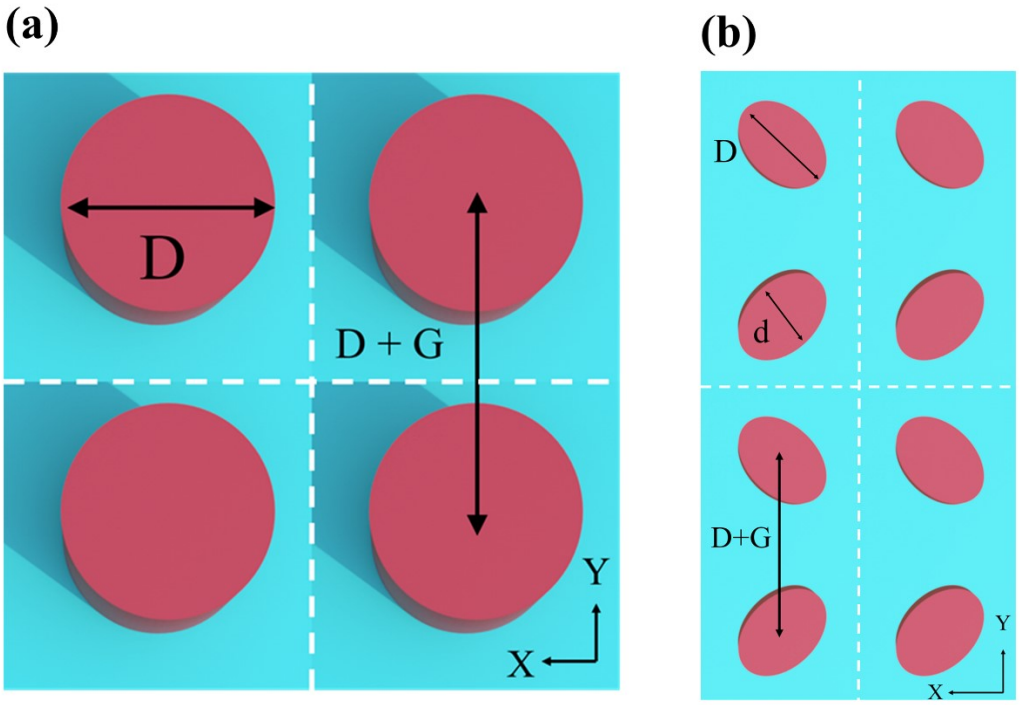

Figure S4. Schematic illustration of the in-plane metasurface layout. (a) Top-view of a 2×2 unit-cell array for the isotropic circular nanopillar design. (b) Top-view of a 2×2 unit-cell array for the proposed elliptical nanopillar design.

The white dashed lines indicate the boundaries of the periodic unit cells. In the proposed design (b), each unit cell comprises two elliptical nanopillars oriented orthogonally (45° and 135°) to break the in-plane symmetry while compensating for polarization sensitivity.

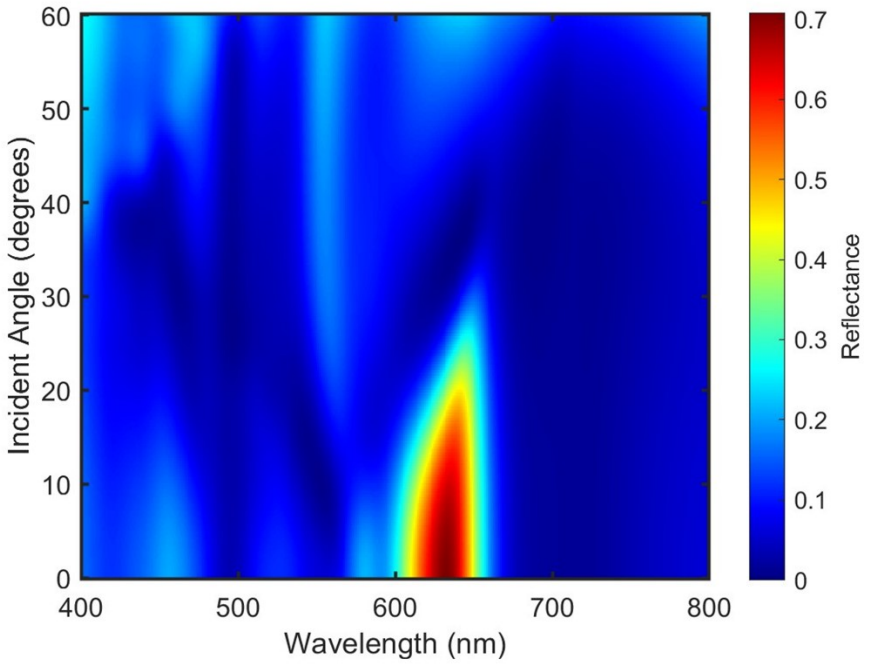

Figure S5. Angular dependence of the reflection spectra for the metasurface.

Spectral evolution of the representative green-channel metasurface as a function of the incident angle (θ) from $0° \; to \; 60°$. The color map illustrates the reflectance intensity across the visible spectrum. The simulation was performed using the Broadband Fixed Angle Source Technique (BFAST) to ensure a constant incident angle across the entire wavelength range.

To address the performance of the proposed metasurface in practical optical systems (such as high-NA imaging or focused illumination), we investigated the angular dependence of the reflection spectra. Taking the green-channel metasurface as a representative example, Figure S5 displays the spectral evolution for incident angles ranging from 0° to 60°.

As shown in the figure, the resonance peak exhibits high stability for small to moderate incident angles. Within the range of $0° \; to \; 20°$, the peak wavelength remains substantially stable with negligible shifting, and the reflectance intensity remains high. As the incident angle increases beyond 30°, a typical blue-shift of the resonance is observed, accompanied by a decrease in peak intensity. These results demonstrate that the design is robust and maintains its narrowband filtering characteristics within a practical angular cone, making it well-suited for integration into conventional CMOS image sensors and micro-display systems with standard numerical apertures.